IEEE Access
Multidisciplinary | Rapid Review | Open Access Journal

Received March 17, 2021, accepted March 26, 2021, date of publication March 30, 2021, date of current version April 8, 2021.

Digital Object Identifier 10.1109/ACCESS.2021.3069939

A New Application of Chaos Game Optimization Algorithm for Parameters Extraction of Three Diode Photovoltaic Model

ABDELHADY RAMADAN[1], SALAH KAMEL[1], MAHMOUD M. HUSSEIN[2], AND MOHAMED H. HASSAN[1]

[1]Department of Electrical Engineering, Faculty of Engineering, Aswan University, Aswan 81542, Egypt
[2]Department of Electrical Engineering, Faculty of Energy Engineering, Aswan University, Aswan 81528, Egypt

Corresponding author: Mahmoud M. Hussein (hussein760@gmail.com)

ABSTRACT The precision of the PV model greatly influences the simulation results to enhance the effectiveness of photovoltaic (PV) energy systems. The PV mathematical model is based on a remarkably nonlinear relationship of its I-V characteristic. The data sheets of overall PV cells do not supply complete information of its parameters. This leads to a nonlinear mathematical model of PV with numerous unknown parameters. Consequently, in this paper, a new application of an appropriate optimization algorithm called Chaos Game Optimization algorithm (CGO) is proposed for estimating the unknown parameters of the three-diode (TD) PV model. The simulation results are carried out for PV real cells and PV module which with varying the temperature and irradiation. The proposed model of the PV module is evaluated by matching its results with the actual PV modules experimental results. To confirm the performance of the CGO algorithm in extracting the parameters of the PV model, its results are compared with the most present and robust techniques results in the literature. The results show that the CGO algorithm attains the least Root Mean Square Error (RMSE), the mean and standard deviation as the best solution. In addition, CGO provides the smallest implementation time compared with the other investigated algorithms.

INDEX TERMS Chaos game optimization algorithm, optimization, PV parameter estimation, three-diode model.

I. INTRODUCTION

Solar energy is considered a significant type from the numerous types of renewable energy resources as a result of providing the appropriate environment for its spread around the world and its cleanliness. It is deemed a worthy solution to cope with fossil fuels shortage [1]. Nowadays, PV modules are being introduced into the markets which have high efficiency and little prices motivated by international government subsidies as well as competition among PV manufacturers [2]. For actual implementation of solar PV systems, an accurate simulation must be prepared in advance. Thus, to enhance the performance of PV systems during the procedures of simulation and design, accurate modeling of the PV modules must be prepared. Nevertheless, the modeling of the PV module is an intricate problem as a result of the I-V characteristic behavior, which is known as a nonlinear relationship that is extremely affected by the changing in temperatures and solar radiations [3]–[8]. There are enormous unknown parameters in the I-V mathematical model. Commonly, there are three types of the PV solar cells mathematical model; single diode (SD) model as the simplest one, double diode (DD) model as an elaborated model, and TD model as a more detailed model. SD model is considered a simple and very acceptable degree of accuracy [9], [10]. The I-V characteristic of the SD model has five unknown parameters, and they are the Photo-generated current (Iph); the diode saturation current (I0); the factor of ideality (a); the series resistance (R_s); and shunt resistance (R_{sh}) [11]. Nevertheless, the SD model has a deficiency of accuracy in the case of the open-circuit voltage with low radiation because of the neglecting of the losses of carrier recombination in the depletion region [12], [13]. To vanquish this problem, the DD model is presented. Another diode is added to show the losses

The associate editor coordinating the review of this manuscript and approving it for publication was Lorenzo Ciani.

of recombination. The DD model presents more precision but this model is more complicated due to the increase of unknown parameters; saturation current and ideality factor parameters of the other diode are added to the unknown parameters in the SD case [13]–[15]. The TD model as a more detailed model is a significant aspect to cope with low radiation conditions in massive PV installations [16]. This model deals with the special effects of leakage current and the boundaries [17]. Although this model can fulfill most of the PV solar cell physical requirements, it includes the calculation of nine parameters and this makes the TD model more complex than SD and DD models [18].

Knowing the values of the PV cell parameter is considered a problem of optimization. There are numerous optimization methods have been proposed for the identification of the PV solar cell unknown parameters. These techniques can be divided into two classifications; conventional algorithms and meta-heuristic algorithms. Several types of the conventional methods have been presented in [19]–[21] for DD model and for TD model in [17]. Nevertheless, these algorithms consume more time and fail their capability to provide precise solutions particularly with an increasing number of unknown estimated parameters [22]. Thus, meta-heuristic algorithms are considered a better solution to avoid the disadvantages of conventional algorithms. The most recent literature for the meta-heuristic algorithms for estimating the unknown PV model parameters is as the following: Bacterial Foraging (BF) algorithm has been presented in [23] that is executed under normal and shading conditions. In [24] Generalized Oppositional Teaching Learning Based Optimization (GOTLBO) has been developed to achieve the optimum solution in little time consuming. In [25], [26], A Differential Evolution with Integrated Mutation per iteration (DEAM) and Hybrid Evolutionary algorithm (DEIM) have been suggested, respectively, that have presented a worthy execution time of CPU and get a good precision. In [1], the Flower pollination algorithm has exhibited unobserved divergence between the estimated and the experimental (I-V) curves, particularly with low solar radiation levels. Additionally, Pattern Search technique [27], Simulated Annealing algorithm (SA) [4], Harmony Search based algorithm (HS) [28], Artificial Bee Swarm Optimization algorithm (ABSO) [29], Artificial Bee Colony algorithm (ABC) [30], Modified Gradient-Based Optimizer (MGBO) [41], an enhanced teaching-learning-based optimization (ETLBO) [42], and Mutative-scale Parallel Chaos Optimization algorithm (MPCOA) [31] are presented to estimate the unknown parameters of SD and DD depending on an experimental data that presented in [32]. In [33], Genetic algorithm is executed to estimate the global optimum unknown parameters for SD and DD. Furthermore, in [34], Bird Mating (BM) algorithm is used to extract the SD unknown parameters for a PV solar array.

From the above literature, it is noticed that most researches are utilizing the common types of PV cell models such as SD and DD. The complex model such as TD is rarely used in modern investigations to evade extracting a higher number of unknown parameters. Nevertheless, it has been confirmed in this research that this model is more efficacious for coping with the more intricate physical attitude of the PV module. Furthermore, the results were less accurate and time consuming for the estimation process when the researchers used the TD model and their research depend on the traditional algorithms [17]. Consequently, a more effective algorithm should be proposed to extract the unknown parameters of this complicated model with more precision and with minimum time consuming.

In this paper, The TD model which is considered the more complicated model is investigated based on two sources of data. The application is the experimental data for 57 mm diameter commercial silicon R.T.C France solar cell. The other one is experimental data measured at the laboratory for PV module Photowatt-PWP201. The main contributions of this work can be shortened as follows:

- The CGO optimization algorithm is applied for accurately and reliably identification the parameters of PV models with the TD using the measured I-V curves.
- The performance and results of the CGO are compared to the recent and efficient algorithms proposed in the literature.
- For more validation of the results, an evaluation analysis which includes RMSE, absolute output current error, and absolute power error are performed.
- The results demonstrate that the CGO technique has more accurate results with the best execution time when compared to the other compared algorithms.

The rest of the paper is arranged as follow: Section 2 presents the mathematical Model of the PV module. The problem formulation is discussed in section 3. Section 4 discusses the theory of the CGO technique. The simulation results are presented in section 5. The conclusion is added in section 6.

II. MATHEMATICAL MODEL

There are numerous mathematical models of the PV module that depict its process and the actual performance. It is becoming essential to achieve this actual behavior of solar cell. Therefore, a detailed model such as TD model is highly recommended to represent the effect of leakage current and boundaries [15], [16] and [36].

1) THE THREE DIODE (TD) MODEL

Fig. 1 shows the TD model that is represented by the I_{ph} shunted with three parallel diodes (D_1, D_2 and D_3) and R_{sh} and series with R_s. The current I_{D1} pass through the diode D_1 indicates the current as a result of recombination and diffusion in the quasi-neutral regions of the bulk regions and the emitter of the P-N junction. The current I_{D2} pass through the diode D_2 indicates the current as a result of recombination in the space charge regions [36]–[38]. The current I_{D3} pass through the diode D_3 designates the impact of the large

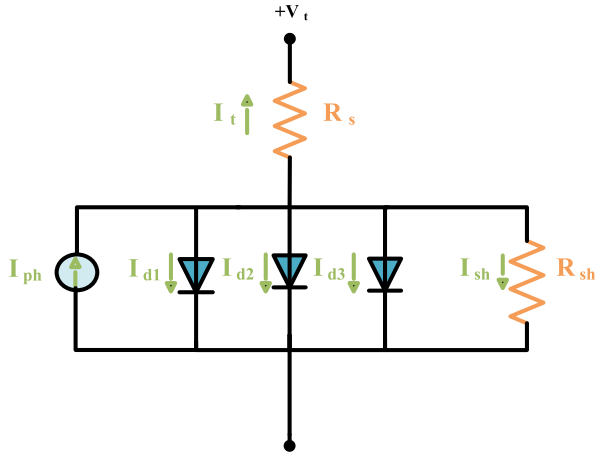

FIGURE 1. TD model mathematical model.

leakage current and the grain boundaries. The R_{sh} is used to calculate the leakage current. Furthermore, the R_S represents the material resistance of the PV cell [1]. So in this model, the PV output current for SD and DD are presented in equation 1 and 2.

$$I_{Out} = I_{Ph} - I_{D1} - I_{sh} \tag{1}$$

$$I_{Out} = I_{Ph} - I_{D1} - I_{D2} - I_{sh} \tag{2}$$

The detailed model of TD is counted as follows

$$I_{Out} = I_{Ph} - I_{D1} - I_{D2} - I_{D3} - I_{sh} \tag{3}$$

$$\begin{aligned} I_{out} = {} & I_{Ph} - I_{sd1}\left[\exp\left(\frac{q\left(V_{out} + I_{out}R_S\right)}{N_1 KT}\right) - 1\right] \\ & - I_{sd2}\left[\exp\left(\frac{q\left(V_{out} + I_{out}R_S\right)}{N_2 KT}\right) - 1\right] \\ & - I_{sd3}\left[\exp\left(\frac{q\left(V_{out} + I_{out}R_S\right)}{N_3 KT}\right) - 1\right] \\ & - \frac{V_{out} + I_{out}R_s}{R_{sh}} \end{aligned} \tag{4}$$

where

I_{sd3} is the saturation current of D_3

N_3 is and ideality factor of D_3.

Some parameters modify as temperature and radiation change according to the following equations:

$$I_{Ph} = \left(I_{Phs} + K_i \Delta T\right)\frac{G}{G_s} \tag{5}$$

$$I_{sd} = I_{sds}\left(\frac{T}{T_s}\right)^3 \exp\left[\frac{q \times E_g}{a \times K}\left(\frac{1}{T_s} - \frac{1}{T}\right)\right] \tag{6}$$

$$E_g = E_{gs}\left(1 - 0.0002677\Delta T\right) \tag{7}$$

$$R_{sh} = R_{shs}\frac{G}{G_s} \tag{8}$$

where I_{Phs}, G_s, I_{sds}, E_{gs}, T_s, and R_{shs} are represented the generated photocurrent, solar radiation, the saturation current, band gap of the PV material, cell absolute temperature, and the shunt resistance of the circuit at the standard test condition (STC), respectively. The value of E_{gs} is 1.121 eV for the silicon cells [39], ΔT is the difference temperature between T_s and T. K_i is the short circuit current coefficient.

TABLE 1. Parameter lower and upper constrains.

Parameter	Solar Cell		PV module	
	Lower Value	Upper Value	Lower Value	Upper Value
Rs	0	0.5	0	2
Rsh	0	100	0	1000
Iph	0	1	0	2
Id1	0	1	0	1
Id2	0	1	0	1
Id3	0	1	0	1
n1	1	2	1	50
n2	1	2	1	50
n3	1	2	1	50

III. THE PROBLEM FORMULATION

The essential purpose of presenting a model of PV solar cell is to reduce the variance between the estimated data and the experimental behavior with different ecological conditions by estimating the optimum values for the anonymous parameters of the PV cell model.

To fulfill the main requirements for the application of any optimization algorithm by defining the solution vector (X), the range of the search, and the objective function [1].

The vector of solutions for TD PV model is realized as the following; X = (R_S, R_{sh}, I_{ph}, I_{sd1}, I_{sd2}, I_{sd3}, N_1, N_2, and N3). The search range (lower and upper boundaries) of the unknown parameters In line with previous literature is speechified, in Table1.

The purpose of the objective function is to diminish the (RMSE) between estimated PV cell model and its experimental values [22]. The current error I_{err} is the variance between the estimated and the experimental currents. The power error P_{err} is the variance between the estimated and the experimental power. I_{err} and P_{err} can be calculated as the following:

$$I_{err} = I_{out} - I_{out-exp} \tag{9}$$

$$P_{err} = P_{out} - P_{out-exp} \tag{10}$$

where I_{out} is the estimated value of the output current that can be calculated from (4) for TD model of the PV cell model.

This objective function is addressed by the following equation:

$$RMSE = \sqrt{\frac{1}{N}\sum_{i=1}^{N} J_i^2\left(V_{out}, I_{out}, X\right)} \tag{11}$$

where N represents the number of the measured data.

The suggested optimization techniques (CGO), improved Grey wolf optimizer (IGWO), manta ray foraging optimization (MRFO), Generalized Predictive Control (GPC), Honey Bee Optimization (HBO) and Arithmetic Optimization Algorithm (AOA)) are mostly utilized to optimal estimation of the unknown parameters for the TD model with minimum error of objective function (RMSE).

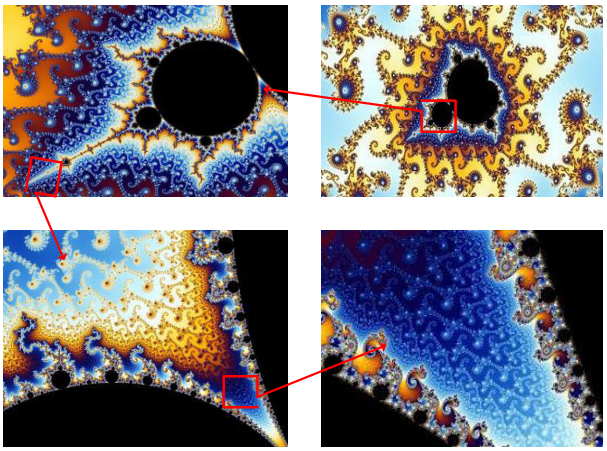

FIGURE 2. Mandelbrot group self-similarity in diverse ranges [3].

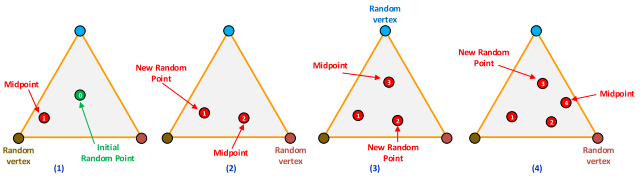

FIGURE 3. Constructing sierpinski triangle using chaos game methodology [35].

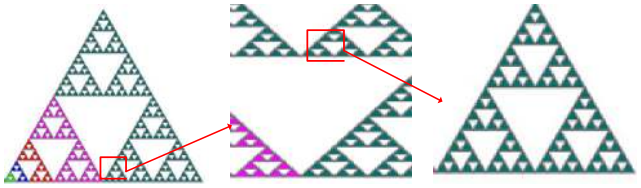

FIGURE 4. The self-similarity of sierpinski triangle in its final form with various ranges [35].

IV. METHODOLOGY

A. CHAOS GAME OPTIMIZATION (CGO)

The essential idea of the CGO algorithm depends on certain rules of chaos theory where the arrangement of fractals by chaos game idea and the fractals self-similarity concerns are in perspective [35]. Chaos theory focuses on some properties in dynamic systems, and these properties are very sensitive to their initial conditions. Despite the randomness present in these dynamic systems, chaos theory indicates that there are some elementary patterns, for example, similar loops, repeating shapes, fractals, and multiple subsystems in the performance of these dynamic systems, so they can be described as self-similar and self-organizing dynamic systems. The generality of the chaotic procedures has graphical forms of fractals. A fractal, in math, is a subgroup of Euclidean space in which a particular geometric form is repetitive in various ranges. The well-known fractals similarity of the Mandelbrot group is drawn in diverse ranges as shown in Fig. 2.

Chaos theory poses that slight variations in the initial conditions for a dynamic system will lead to some severe differences in the coming conditions of these systems because of their reliance on its initial conditions. According to this theory, the current condition of a system can determine the subsequent state of that system while the approximate current condition of the system does not roughly define the subsequent condition of that system. The chaos game, in math, is the approach of producing fractals exploiting a primary polygon form and a randomly nominated primary point. The essential objective is to construct a concatenation of points in a repeated attitude to attain a shape that has a similar form in diverse ranges.

To understand the approach of the chaos game, a simple example can be taken to construct a Sierpinski triangle as a straightforward fractal. Initially, three vertices are nominated to construct the main fractal shape that results in a triangle in this situation. Every vertex from nominated vertices is highlighted in one of the colors red, green and blue. In this case, a die used must have two sides in red color, two sides in blue color and two sides in green color. A first random point is nominated as the initial point of the fractal that is deemed in this case as a seed. As the die rolls and depending on the color that appears, the seed is moved from the first point towards the relevant vertex midway the space between the vertex and the seed. When the die is rolled again, the new location of the seed is exploited as the beginning point in the next reiteration and consequently, the seed is shifted into the intentional vertex. The Sierpinski triangle is accomplished as the final form when the die is rolled several times. Fig. 3 indicates the schematic view of the CGO approach while Fig. 4 presents the self-similarity of Sierpinski triangle in its final form with various ranges.

B. MATHEMATICAL MODEL

The CGO algorithm has been discussed which depends on the principles of chaos theory. The main conceptions of the chaos game theory and fractals are exploited to formulate the CGO algorithm mathematical model. Due to the numerous algorithms inspired from the natural evolution, a set of solutions are developed in random modifications and selection, the proposed CGO algorithm deems a number of candidate solutions (X) in this target which signifies some of the eligible points within the triangle of Sierpinski. Each solution candidate (X_i), involves some decision variables ($x_{i,j}$) that represents the location of these eligible points inner the triangle of Sierpinski. In the CGO optimization algorithm, the triangle of Sierpinski is deemed as a search area for solution candidates. The following equation indicates the mathematical model of these concepts:

$$X = \begin{bmatrix} X_1 \\ X_2 \\ . \\ . \\ X_i \\ . \\ . \\ X_n \end{bmatrix} = \begin{bmatrix} x_1^1 & x_1^2 & \ldots.. & x_1^j & \ldots.. & x_1^d \\ x_2^1 & x_2^2 & \ldots.. & x_2^j & \ldots.. & x_2^d \\ . & . & & . & & . \\ . & . & & . & & . \\ x_i^1 & x_i^2 & \ldots.. & x_i^j & \ldots.. & x_i^d \\ . & . & & . & & . \\ . & . & & . & & . \\ x_n^1 & x_n^2 & \ldots.. & x_n^j & \ldots.. & x_n^d \end{bmatrix},$$

$$\begin{cases} i = 1, 2, \ldots., n \\ j = 1, 2, \ldots.., d \end{cases} \quad (12)$$

where:

n refers to the eligible points number (solution candidates) within the triangle of Sierpinski (search area).

d refers to the points dimension.

The first locations of the eligible seeds are randomly located within the search range as the following:

$$x_i^j(0) = x_{i,min}^j + rand.\left(x_{i,max}^j - x_{i,min}^j\right), \quad \begin{cases} i = 1, 2, \ldots., n \\ j = 1, 2, \ldots.., d \end{cases} \quad (13)$$

where:

$x_i^j(0)$ Calculates the eligible points first location, *rand* refers to a range of number values with in [0, 1].

$x_{i,min}^j$ And $x_{i,max}^j$ refer to the lowest and highest permissible values for the j^{th} decision variable of the i^{th} solution candidate.

As described above, the essentials of chaos theory relate to the presence of certain elementary patterns in the attitude of dynamic systems that assort these systems in self-organized and self- similar systems. The initial points that randomly formed are considered as eligible points; it represents the basic forms of dynamic systems depending on the chaos theory. In order to deem these eligible points as basic forms of dynamic systems appearing the self-similarity, it is mathematically modeled by deeming the superiority of the candidates of the solution (X). The candidates of solution with the uppermost and lowermost levels of eligibility are equipollent to the greatest and poorest values of fitness for overall solution candidates, respectively. The core idea of this model is to produce various eligible points within the search area to complete the entire form of the Sierpinski Triangle. Regarding to this, the approach for constructing new points within the triangle of Sierpinski as shown in Fig. 4 is employed for this target. For every initial eligible point in the search area (X_i), an interim triangle is sketched and considered with three points as the following:

– GB: Global Best position of the so far,

– MG_i: Mean Group position,

– X_i: i^{th} is the solution candidate position as the chosen initial eligible point.

The GB denotes the away far found best solution candidate that has the highest level of eligibility and MG_i denotes the average values of various randomly chosen initial eligible points with a similar probability of involving the present deemed initial eligible point (X_i). GB and MG_i combined with the nominated initial eligible point (X_i) are deemed as the triangle of Sierpinski three vertices. As declared earlier, for every initial eligible point within the search range, an interim triangle is formulated with the aim of constructing various new points within the search area that could be deemed as the new eligible points for finishing the Sierpinski triangle points. Fig. 5 shows a schematic view of constructing interim triangles while Fig. 6 provides a supplementary detailed schematic depiction of this purpose.

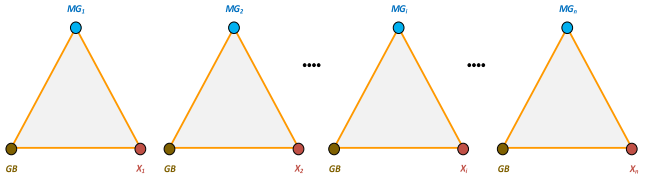

FIGURE 5. Constructing interim triangles schematic view [35].

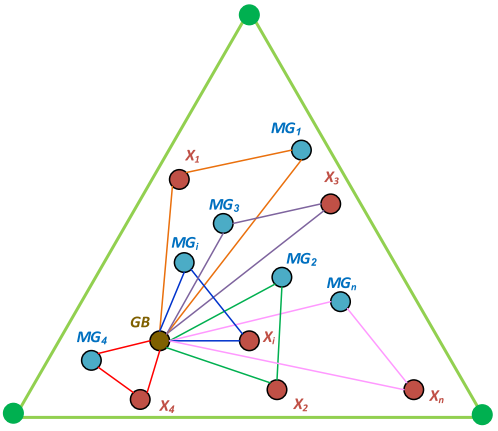

FIGURE 6. Interim triangles within the search area schematic view [35].

The basic target from constructing the temporary triangles is to produce new points with the search range that could have the opportunity to be the new eligible points. Four methods are described to accomplish this objective. This procedure is characterized for the i^{th} interim triangle containing the i^{th} initial eligible point while the identical procedure is iterated for overall the eligible points and interim triangles within the search range.

About the i^{th} interim triangle, the Sierpinski triangle three vertices within the search range including three i^{th} starting eligible point; the green point (GB), blue point (X_i) and red point (MG_i). A die and three seeds are exploited for forming new points according to the chaos game approach in this interim triangle. The first, the second and the third seeds are positioned in X_i, GB and MG_i, respectively. With regard to the first seed that is located in the X_i, a die that has three red sides and three green sides are exploited. When the die is rolled and based on the color that appears (green or red), the seed is moved in Xi in the direction of GB (green face) or MGi (red face). Whenever rolling the die and depending on the color that appears (red or green), the seed in X_i is shifted to the GB (green side) or MG_i (red side). This feature can be modeled through a certain random integer producing function that constructs just two integers [0 and 1] for the opportunity of choosing red or green sides. When the green side appears, the seed located in the X_i is shifting on the way to the GB but when the red side appears,

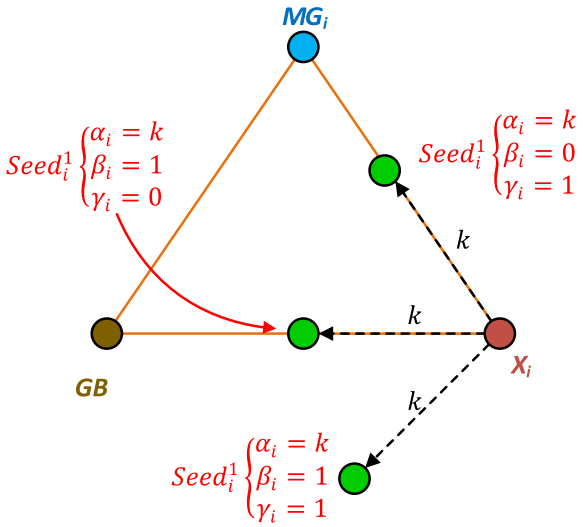

FIGURE 7. The presentation of schematic updated location for the first seed within the search area [35].

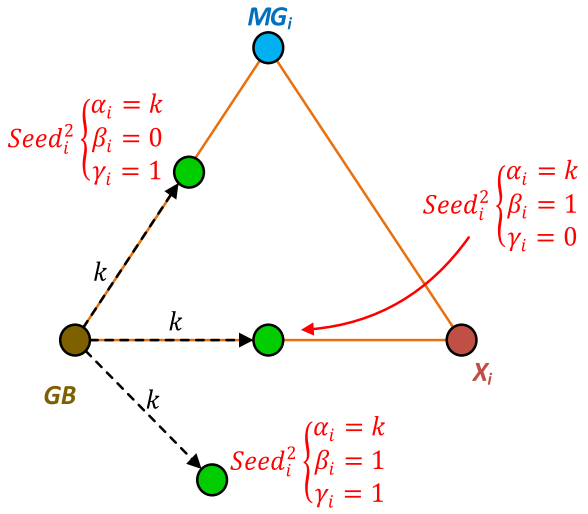

FIGURE 8. The presentation of schematic updated location for the second seed within the search area [35].

the seed located in the X_i is shifting on the way to the MG_i. Irrespective of the reality that each of the red or green sides have an equivalent probability of appearing in this game, the possibility of constructing two random integers for both MG_i and GB are also deemed that the seed located in the X_i is shifted along the way of the linked lines between the MG_i and the GB. Several randomly produced factorials are also exploited depending on the reality of the motion of the seeds within the search area must be restricted due to the chaos game procedure that controls this feature. Fig. 7 describes a schematic presentation of this procedure for the first seed whilst the mathematical presentation for it is as the following:

$$seed_i^1 = X_i + \alpha_i \times (\beta_i - GB - \gamma_i \times MG_i), \quad i = 1, 2, \ldots, n \tag{14}$$

where:

X_i refers to the solution candidate (i^{th}).

GB refers to the so far global solution.

MG_i refers to the average values of certain starting eligible points that are deemed as three vertices in the i^{th} interim triangle.

α_i refers to the randomly produced factorial for modeling the seeds motion limitations.

β_i and γ_i refer trandom integer of 0 or 1 for modeling the rolling a die probability.

With regard to the second seed that is located in the GB, a die has in this case three sides in blue color and three sides in red color are exploited. With rolling the die and depending on the color that appears (red or blue), the seed in the GB is shifted to the X_i (blue side) or the MG_i (red side). This feature can be modeled in a random certain integer production function that produces just two integers as 0 and 1 for the opportunity of choosing red or blue sides. The location of the seed in the GB is shifted to the X_i when the blue side appears, whilst the location of the seed in the GB is shifted to the MG_i when the red side appears. Irrespective of the reality that each blue side or red side has an equivalent probability of appearing in this game, the possibility of constructing two random integers of 1 for X_i and MG_i are also deemed that the seed located in GB is shifted along the way of the linked lines between MG_i and X_i. Depending on the reality of the seed movement within the search area ought to be restricted according to the chaos game procedure; certain randomly produced factorials are exploited to control this feature. Fig. 8 describes a schematic presentation of this procedure for the second seed whilst the mathematical presentation for it is as the following:

$$seed_i^2 = GB + \alpha_i \times (\beta_i \times X_i - \gamma_i \times MG_i), \quad i = 1, 2, \ldots, n \tag{15}$$

Also, for the third seed that is located in MG_i, a die has in this case three sides in blue and three sides in green are exploited. With rolling the die and depending on the color that appears (green or blue), the seed in MG_i is shifted to the GB (green side) or the X_i (blue side). This feature can be modeled through a certain random integer production function that produces just two integers as 0 and 1 for the opportunity of choosing green or blue sides. The location of the seed in the MG_i is shifted to the X_i when the blue side appears, whilst the location of the seed in the MG_i is shifted to the GB when the green side appears. Irrespective of the reality that each of the green or blue sides have an equivalent probability of appearing in this game, the possibility of constructing two random integers of 1 for both X_i and GB are also deemed that the seed located in the MG_i is shifted along the way of the linked lines between the GB and the X_i. Depending on the reality of the seed movement within the search area ought to be restricted according to the chaos game procedure; certain randomly produced factorials are exploited in this purpose to control this feature. Fig. 9 describes a schematic presentation of this procedure for the third seed whilst the mathematical

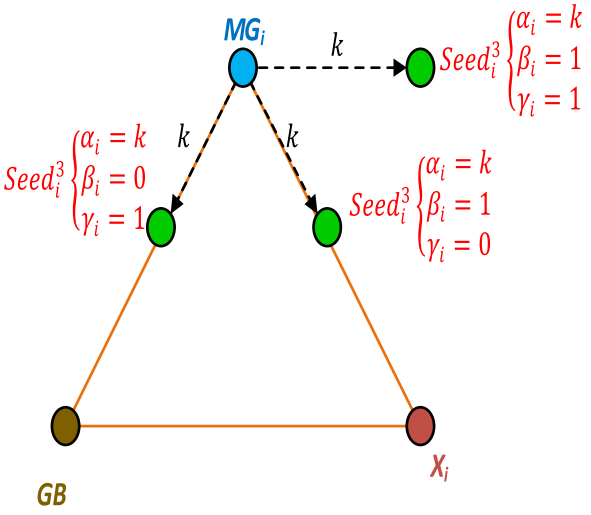

FIGURE 9. The presentation of schematic the updated location for the third seed within the search area [35].

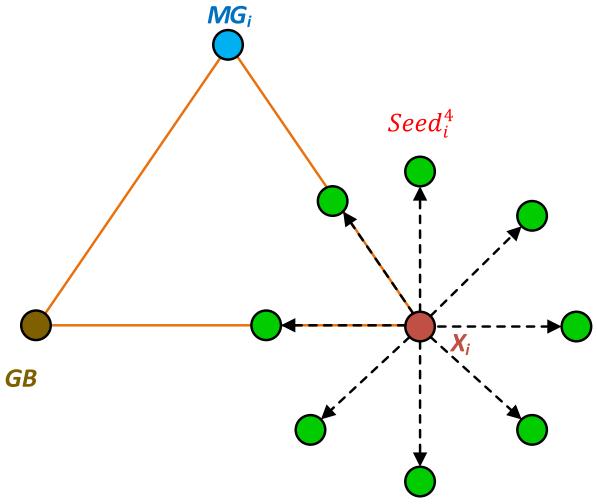

FIGURE 10. The presentation of schematic updated location for the fourth seed within the search area [35].

presentation for it is as the following:

$$seed_i^3 = MG_i + \alpha_i \times (\beta_i \times X_i - \gamma_i \times GB), \quad i = 1, 2, \ldots, n \tag{16}$$

To carry out the phase of mutation in the location updates of the starting eligible points within the search range, the extra seed is also exploited as a fourth seed that is located in the X_i. The location updating procedure for the fourth seed is determined depending on certain random variations in the randomly selected decision variables. Fig. 10 describes a schematic presentation of this procedure for the fourth seed whilst the mathematical presentation for it is as the following:

$$seed_i^4 = X_i \left(x_i^k = x_i^k + R\right), \quad k = [1, 2, \ldots, d] \tag{17}$$

where:

k refers to an integer in random range of [1, d]

Algorithm: CGO Algorithm
Determine random values for starting locations (x_i^j) of the eligible points (X_i)
Estimate objective function for every eligible point
GB = the best eligible point so far
while (t < maximum iterations number)
for i=1: number of sarting eligible points
Determine MG_i
Determine an interim triangle with X_i, MG_i, and GB.
Calculate the values of α_i, β_i, and γ_i
Calculate new seeds by Eqs. 14 to 17.
if the new seeds break the allowable boundary range
Control the location restrictions for new seeds and correct it
end if
Estimate objective function for the new seeds
if the objective function of the new seeds better than objective function of the starting seeds
replace the worst starting eligible points by the new seeds
end if
modify GB if a superior solution is obtained it
end for
t=t+1
end while
back to GB
end process

FIGURE 11. The CGO algorithm pseudo-code.

R refers to an uniformly random number that distributed in range of [0,1].

In the suggested CGO algorithm, for controlling and adjusting the rate of exploration and exploitation, four equations are exploited to determine the α_i, as indicated in Eq. (18), that is used for modeling the seeds motion restrictions. To determine the location of the first to third seeds, these four equations are used randomly.

$$\alpha_i = \begin{cases} Rand \\ 2 \times Rand \\ (\delta \times Rand) + 1 \\ (\varepsilon \times Rand) + (\varepsilon) \end{cases} \tag{18}$$

where:

Rand refers to a random number distributed uniformly within range [0,1].

δ and ε refer to integers random values within range [0,1].

Depending on the matter of the self-similarity in the fractals, the initial eligibility points together with the newly generated seeds using the conception of the chaos game must be deemed to select whether the newly produced seeds ought to

TABLE 2. Estimated parameter in case of the TD model obtained by different optimization algorithms.

Algorithm	CGO	IGWO	MRFO	GPC	HBO	AOA
Rs (Ω)	0.036743	0.020667781	0.03156444	0.03	0.045132	0.03
Rsh(Ω)	55.50803	56.61265221	59.39127188	12.81199401	59.99766	60
Iph(A)	0.760781	0.763766962	0.762827567	0.355884681	0.762158	0.739783472
Isd1(A)	7.13E-07	2.61E-06	1.43E-07	1.00E-10	4.15E-06	1.00E-10
Isd2(A)	5.18E-08	2.51E-06	1.03E-06	1.00E-10	1.00E-10	1.00E-10
Isd3(A)	2.26E-07	1.25E-06	4.03E-07	1.00E-10	1.00E-10	1.00E-10
N1	1.999998	1.964211911	1.942349179	1	1.931285	1
N2	2	1.90492046	1.830518992	1	1.01184	1
N3	1.44682	1.718822839	1.52302743	1	1	1
RMSE	0.0009824174	0.0074073	0.0028391	0.064496	0.002141689	0.065816

TABLE 3. Statistical results of CGO and other recent algorithms.

Algorithm	Minimum	Average	Maximum	STD
CGO	0.000982	0.000982	0.000982	1.24841E-09
IGWO	0.00528	0.006115	0.007407	0.001134872
MRFO	0.002038	0.002526	0.002839	0.000428371
GPC	0.063645	0.06421	0.064496	0.000489602
HBO	0.001493	0.001961	0.002247	0.000408241
AOA	0.061794	0.06722	0.074049	0.006246917

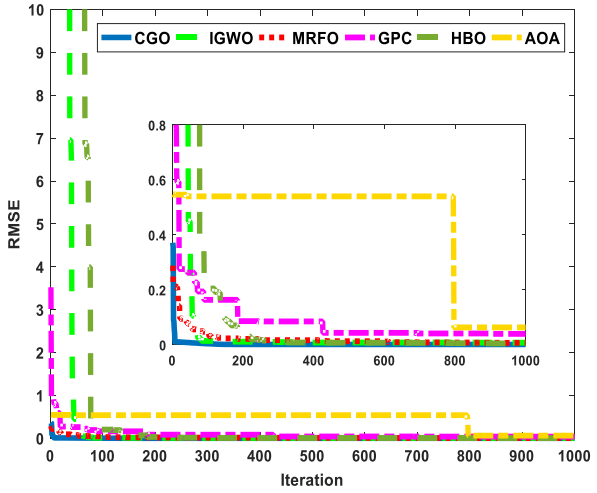

FIGURE 12. Convergence curve of CGO and all compared Algorithms for TD model.

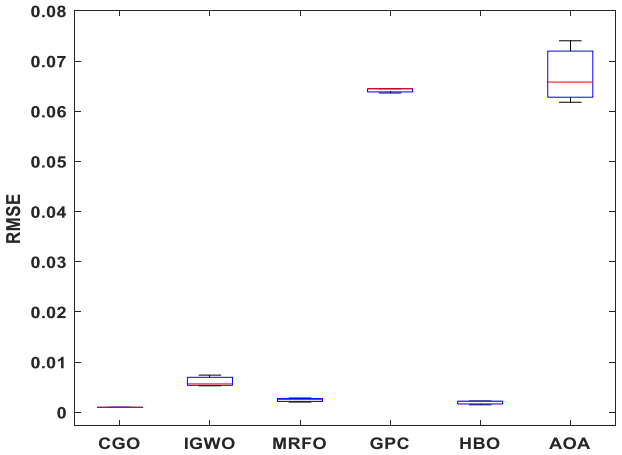

FIGURE 13. Boxplot for statistical results of different algorithms.

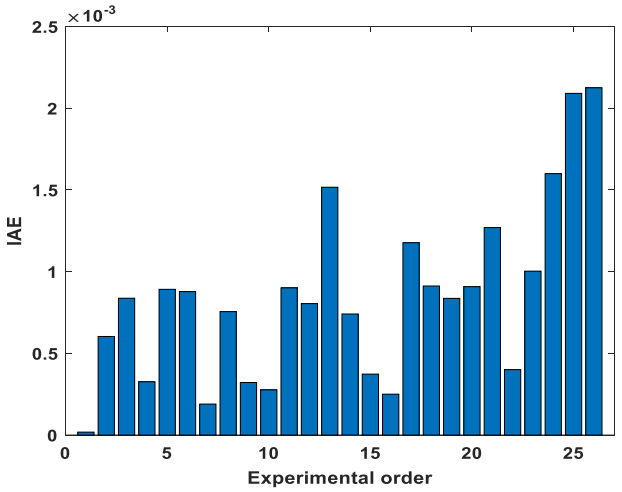

FIGURE 14. Current absolute error.

be involved or not with the overall eligible points within the search range. The new candidate solutions are compared to the initial points, so that the initial points (seeds) are replaced by the new points, in the event that the new points reach the best levels of self-similarity or reservation of the initial points in the event that the worst level of self-similarity is reached with using the new points This must be taken into account that the replacement procedure is executed in the mathematical methodology to get model in less complexity. Actually, overall eligible points that are so far found in the search area are exploited to complete the total form of the Sierpinski triangle. It is important to deal with solution variables (x_i^j) that violate the boundary ranges of the variables. In this case, a mathematical flag is realized that the x_i^j is outside the range of variables, the flag instructs to change the boundaries of the violating variables. The end criterion is considered based

TABLE 4. Voltage, current and power experimental, simulated and the absolute errors values using CGO for the TD model.

V_{out_exp}	I_{out_exp}	I_{out}	I_{err}	IAE	P_{out_exp}	P_{out}	P_{err}	PAE
-0.2057	0.764	0.7640	0.000018	0.000018	-0.157155	-0.157151	-0.000004	0.000004
-0.1291	0.762	0.7626	-0.000603	0.000603	-0.098374	-0.098452	0.000078	0.000078
-0.0588	0.7605	0.7613	-0.000837	0.000837	-0.044717	-0.044767	0.000049	0.000049
0.0057	0.7605	0.7602	0.000326	0.000326	0.004335	0.004333	0.000002	0.000002
0.0646	0.76	0.7591	0.000892	0.000892	0.049096	0.049038	0.000058	0.000058
0.1185	0.759	0.7581	0.000878	0.000878	0.089942	0.089837	0.000104	0.000104
0.1678	0.757	0.7572	-0.000190	0.000190	0.127025	0.127056	-0.000032	0.000032
0.2132	0.757	0.7562	0.000755	0.000755	0.161392	0.161231	0.000161	0.000161
0.2545	0.7555	0.7552	0.000322	0.000322	0.192275	0.192193	0.000082	0.000082
0.2924	0.754	0.7537	0.000276	0.000276	0.220470	0.220389	0.000081	0.000081
0.3269	0.7505	0.7514	-0.000901	0.000901	0.245338	0.245633	-0.000294	0.000294
0.3585	0.7465	0.7473	-0.000804	0.000804	0.267620	0.267909	-0.000288	0.000288
0.3873	0.7385	0.7400	-0.001517	0.001517	0.286021	0.286608	-0.000587	0.000587
0.4137	0.728	0.7273	0.000741	0.000741	0.301174	0.300867	0.000307	0.000307
0.4373	0.7065	0.7069	-0.000373	0.000373	0.308952	0.309116	-0.000163	0.000163
0.459	0.6755	0.6752	0.000250	0.000250	0.310055	0.309940	0.000115	0.000115
0.4784	0.632	0.6308	0.001177	0.001177	0.302349	0.301786	0.000563	0.000563
0.496	0.573	0.5721	0.000912	0.000912	0.284208	0.283756	0.000452	0.000452
0.5119	0.499	0.4998	-0.000836	0.000836	0.255438	0.255866	-0.000428	0.000428
0.5265	0.413	0.4139	-0.000908	0.000908	0.217445	0.217923	-0.000478	0.000478
0.5398	0.3165	0.3178	-0.001270	0.001270	0.170847	0.171532	-0.000685	0.000685
0.5521	0.212	0.2124	-0.000400	0.000400	0.117045	0.117266	-0.000221	0.000221
0.5633	0.1035	0.1025	0.001003	0.001003	0.058302	0.057737	0.000565	0.000565
0.5736	-0.01	-0.0084	-0.001600	0.001600	-0.005736	-0.004818	-0.000918	0.000918
0.5833	-0.123	-0.1251	0.002091	0.002091	-0.071746	-0.072966	0.001220	0.001220
0.59	-0.21	-0.2079	-0.002125	0.002125	-0.123900	-0.12265	-0.00125	0.001254

TABLE 5. Estimated parameter in the case of TD model obtained by different optimization algorithms.

Algorithm	CGO	IGWO	MRFO	GPC	HBO	AOA
Rs (Ω)	1.201271	1.175465	1.220382	1	1.193227	1
Rsh(Ω)	981.9828	938.932	729.2449	68.92569	1000	1000
Iph(A)	1.030514	1.03142	1.032894	1.142153	1.030764	0.94814
Isd1(A)	4.25E-09	5.56E-07	5.01E-07	1.26E-07	1.00E-10	1.00E-10
Isd2(A)	4.50E-10	4.37E-08	2.05E-06	1.00E-10	1.00E-10	1.00E-10
Isd3(A)	3.48E-06	3.70E-06	4.36E-07	3.38E-07	3.75E-06	5.20E-06
N1	48.50769	48.7707	49.49202	45.64516	48.8507	50
N2	48.5083	46.34187	48.35934	50	49.03756	50
N3	48.50793	49.49056	45.69006	41.55795	48.79462	50
RMSE	0.0024251	0.0026700	0.0025249	0.039464	0.0024420	0.091061

on the total number of iterations that the optimization procedure ends after a specified number of iterations. The steps CGO algorithm is as the following whilst the pseudo-code of this optimization is indicated in Fig. 11.

Step 1: Using random nomination method to define the initial locations of the solution candidates (X) or the starting eligible points within the search area.

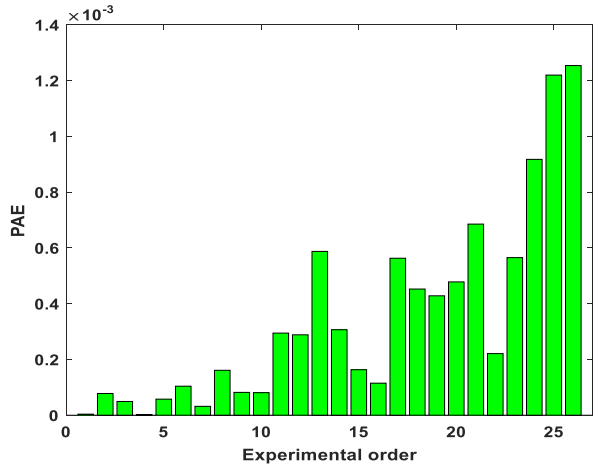

FIGURE 15. Power absolute error.

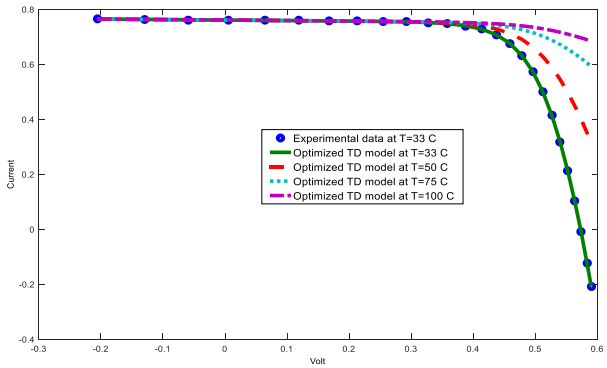

FIGURE 16. The current at different temperature for optimized TD model.

Step 2: Calculate the fitness values of the staring solution candidates depending on the self-similarity of the starting eligible points.

Step 3: Determined the Global Best (GB) that relevant to the point that has high eligibility grade.

Step 4: For every eligible point (X_i) within the search range, determine a Mean Group (MG_i) using a random selection procedure.

Step 5: For every eligible point (X_i) within the search area, determine an interim triangle with specified three vertices of X_i, MG_i, and GB.

Step 6: For every interim triangles, Calculate the values of the α_i, β_i, and γ_i.

Step 7: For every interim triangles, create the four seeds depending on the Eqs. (13)–(16).

Step 8: For the new produced seeds with the x_i^j external the variables scope, conduct a boundary condition check.

Step 9: Calculate the objective function of the new seeds (new solution candidates) depending on the matter of self-similarity.

Step 10: Substitute the initial eligible points by the new seeds when the objective function of the new sees give high self-similarity levels.

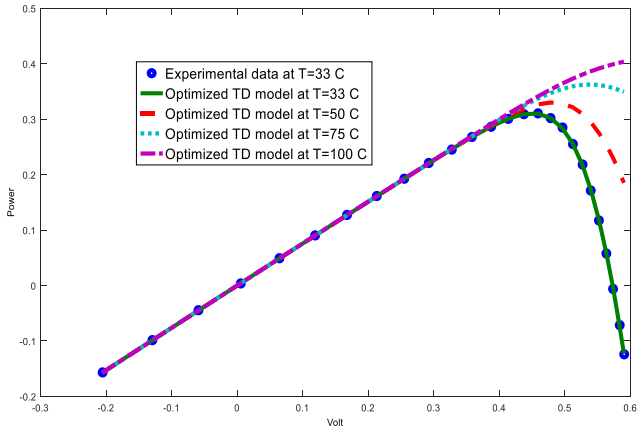

FIGURE 17. The power at different temperature for optimized TD model.

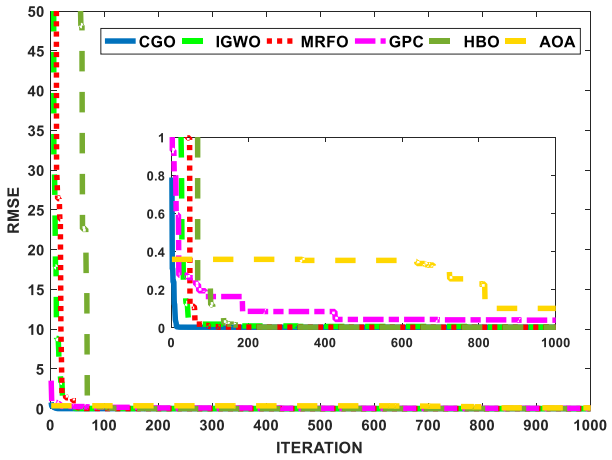

FIGURE 18. Convergence curve of CGO and other compared algorithms for TD model (PV module).

Step 11: Check the terminating criterion according to the specified maximum iteration.

V. SIMULATION RESULTS AND DISCUSSIONS

In this section, CGP is applied to optimize the parameters of the TD model. Part 1 discusses a comparative study between optimized parameters of the TD model obtained by CGO and other recent algorithms for commercial silicon R.T.C France solar cell. Part 2 discusses the application of CGO to estimate the parameters of the TD model for a more complicated real system a polycrystalline PV panel STM6-120/36. The detailed results are presented as follow:

A. PART 1 RESULTS

This part discusses the application of CGO for estimating the parameters of the TD PV model. The real data of 57 mm diameter commercial silicon R.T.C France solar cell (under 1000 W = m2 at 33 °C) is considered in this application [40]. Table 2 presents the nine estimated parameters of the TD model using CGO and other algorithms. The RMSE values obtained using the CGO and other compared

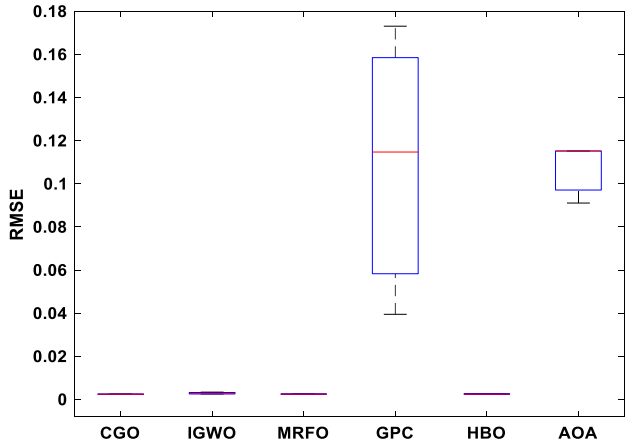

FIGURE 19. Boxplot for statistical results of different algorithms.

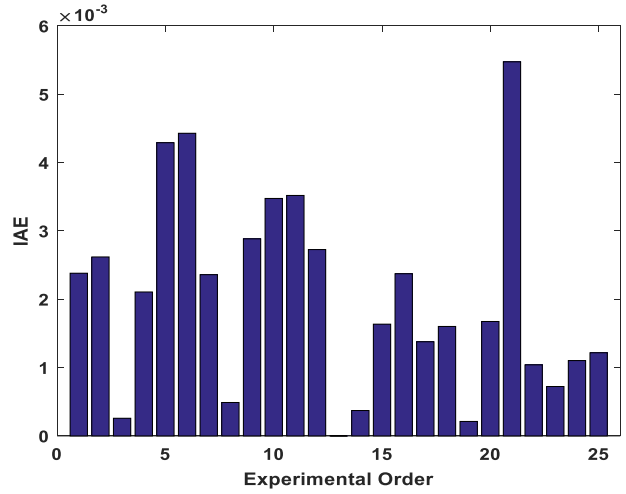

FIGURE 20. The current absolute error.

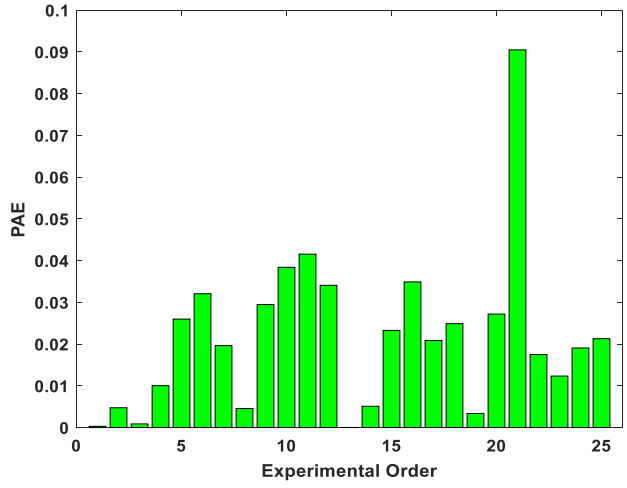

FIGURE 21. The power absolute error.

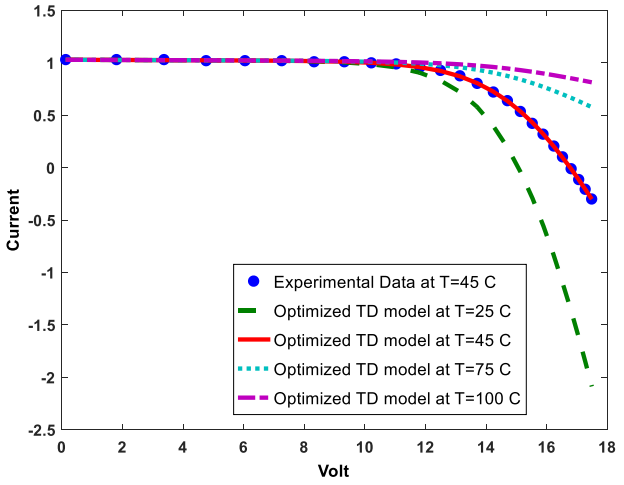

FIGURE 22. Current at different temperature for optimized TD model.

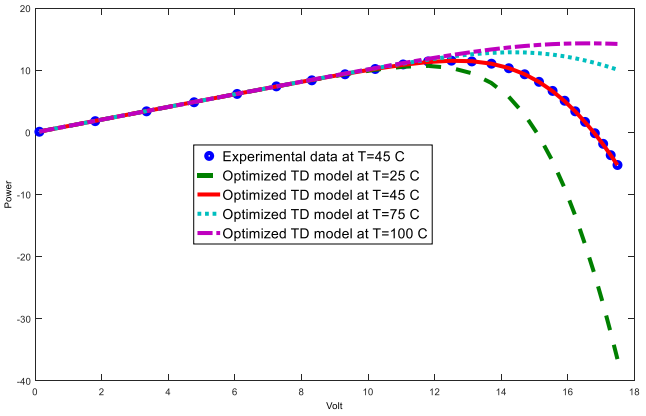

FIGURE 23. Power at different temperature for optimized TD model.

TABLE 6. Statistical results of CGO and other recent algorithms.

Algorithm	Minimum	Average	Maximum	STD
CGO	0.002425075	0.002425092	0.0024251	1.44688E-08
IGWO	0.0025219	0.002856883	0.003378662	0.000457908
MRFO	0.0024265	0.002465567	0.0025249	5.22369E-05
GPC	0.039464	0.109083016	0.17307	0.066980823
HBO	0.002434111	0.002499919	0.002623617	0.000107199
AOA	0.091061	0.107147772	0.115191158	0.013931553

algorithms are also presented in Table 2. From Table 2, the results of the CGO algorithm for the TD model estimated parameter are more accurate in comparison with other algorithms. It is highly clear that the CGO technique gives the least RMSE value. There are many references in the literature that discuss the application of different algorithms on the same example (silicon R.T.C France solar cell). From the authors' point of view, this value is more accurate as to the most general best RMSE value than Single Diode model 9.8600E-04 and 9.8300 E-04 for the double diode model [40]. The speed of CGO is cleared in Fig. 12 which presents the

TABLE 7. Voltage, current and power experimental, simulated and the absolute errors values using CGO for TD model.

V_{out_exp}	I_{out_exp}	I_{out}	I_{err}	IAE	P_{out_exp}	P_{out}	P_{err}	PAE
0.1248	1.0315	1.029119	0.002381	0.002381	0.1287	0.1287	0.1287	0.1287
1.8093	1.03	1.027381	0.002619	0.002619	1.8636	1.8636	1.8636	1.8636
3.3511	1.026	1.025741	0.000259	0.000259	3.4382	3.4382	3.4382	3.4382
4.7622	1.022	1.024107	-0.00211	0.002107	4.8670	4.8670	4.8670	4.8670
6.0538	1.018	1.022291	-0.00429	0.004291	6.1628	6.1628	6.1628	6.1628
7.2364	1.0155	1.019929	-0.00443	0.004429	7.3486	7.3486	7.3486	7.3486
8.3189	1.014	1.01636	-0.00236	0.00236	8.4354	8.4354	8.4354	8.4354
9.3097	1.01	1.010489	-0.00049	0.000489	9.4028	9.4028	9.4028	9.4028
10.2163	1.0035	1.000616	0.002884	0.002884	10.2521	10.2521	10.2521	10.2521
11.0449	0.988	0.984525	0.003475	0.003475	10.9124	10.9124	10.9124	10.9124
11.8018	0.963	0.959481	0.003519	0.003519	11.3651	11.3651	11.3651	11.3651
12.4929	0.9255	0.922773	0.002727	0.002727	11.5622	11.5622	11.5622	11.5622
13.1231	0.8725	0.872499	9.98E-07	9.98E-07	11.4499	11.4499	11.4499	11.4499
13.6983	0.8075	0.807128	0.000372	0.000372	11.0614	11.0614	11.0614	11.0614
14.2221	0.7265	0.728136	-0.00164	0.001636	10.3324	10.3324	10.3324	10.3324
14.6995	0.6345	0.636874	-0.00237	0.002374	9.3268	9.3268	9.3268	9.3268
15.1346	0.5345	0.535878	-0.00138	0.001378	8.0894	8.0894	8.0894	8.0894
15.5311	0.4275	0.429102	-0.0016	0.001602	6.6395	6.6395	6.6395	6.6395
15.8929	0.3185	0.318288	0.000212	0.000212	5.0619	5.0619	5.0619	5.0619
16.2229	0.2085	0.206825	0.001675	0.001675	3.3825	3.3825	3.3825	3.3825
16.5241	0.101	0.095525	0.005475	0.005475	1.6689	1.6689	1.6689	1.6689
16.7987	-0.008	-0.00904	0.00104	0.00104	-0.1344	-0.1344	-0.1344	-0.1344
17.0499	-0.111	-0.11172	0.000723	0.000723	-1.8925	-1.8925	-1.8925	-1.8925
17.2793	-0.209	-0.2101	0.001103	0.001103	-3.6114	-3.6114	-3.6114	-3.6114
17.4885	-0.303	-0.30178	-0.00122	0.001217	-5.2990	-5.2990	-5.2990	-5.2990

convergence curve of the CGO technique and other compared algorithms. To check the robustness of the CGO algorithm, the statistical results of 15 individual runs for all algorithms are tabulated in Table 3. The graphical presentation of the statistical results is presented in Fig. 13 through the boxplot figure. Table 4 gives the value of experimental measurements of voltage, current and power. Also, it presents the current absolute error (IAE) and power Absolute error (PAE) declared by Eq. (19). The IAE and PAE are graphically displayed in Figs. 14 and 15. The current and power curves for different temperature of the estimated TD model are shown in Figs. 16, 17.

$$IAE = \sqrt[2]{(I_{err})^2}, \quad PAE = \sqrt[2]{(P_{err})^2} \tag{19}$$

B. PART 2 (PV MODULE RESULTS)

In this part, the CGO is applied to estimate the parameters of the TD model for the real PV module Photowatt-PWP201 [40]. This module contains 36 polycrystalline silicon cells connected in series and operating at an irradiance of 1000 W/m^2 and temperature of 45C.In the same manner of part 1, the results are arranged as follow:

Table 5 presents the nine estimated parameters of the TD model and the RMSE for CGO and other algorithms. CGO gives the best RMSE and this proves that the proposed technique gives the most accurate TD model parameters. The convergence curve of the CGO when applied to estimate the PV module parameters in comparison with other compared algorithms is presented in Fig.18 that presents the fast response of the CGO algorithm. The statistical results for 15 independent runs for all algorithms are presented in Table 6. The slight change in the RMSE value of CGO during these independent runs is an explicit indication of the robust of CGO in comparison with other algorithms. The boxplot for the statistical results is presented in Fig. 19. Table 7 presents the value of experimental measurements of voltage, current and power. Also, it presents the IAE and PAE. Figs. 20 and 21 display The IAE and PAE. The current and power curves for different temperature of the estimated SD model are presented in Figs. 22 and 23.

VI. CONCLUSION

In this paper, a new application of the Chaos Game Optimization algorithm has been proposed for estimating the parameters of the TD PV model. The TD model has been selected as it is the most detailed model for PV cell. The obtained results of CGO have been compared with other recent optimization algorithms. The results were compared via different evaluation factors such as RMSE values and the statistical analysis also calculating the IAE and PAE values for all the real measured values. For deep check, the CGO has been applied for estimating the parameters of PV module Photowatt-PWP201 contained 36 polycrystalline silicon cells. In all cases, the results obtained by the CGO algorithm were more accurate than those obtained by other optimization algorithms. Moreover, it has a faster response.

REFERENCES

[1] D. F. Alam, D. A. Yousri, and M. B. Eteiba, "Flower pollination algorithm based solar PV parameter estimation," *Energy Convers. Manage.*, vol. 101, pp. 410–422, Sep. 2015.

[2] D. Mathew, C. Rani, M. Rajesh Kumar, Y. Wang, R. Binns, and K. Busawon, "Wind-driven optimization technique for estimation of solar photovoltaic parameters," *IEEE J. Photovolt.*, vol. 8, no. 1, pp. 248–256, Jan. 2018.

[3] M. H. Qais, H. M. Hasanien, S. Alghuwainem, and A. S. Nouh, "Coyote optimization algorithm for parameters extraction of three-diode photovoltaic model of photovoltaic modules," *Energy*, vol. 187, pp. 1–8, Nov. 2019.
[4] K. M. El-Naggar, M. R. AlRashidi, M. F. AlHajri, and A. K. Al-Othman, "Simulated annealing algorithm for photovoltaic parameters identification," *Sol. Energy*, vol. 86, no. 1, pp. 266–274, Jan. 2012.
[5] M. H. Qais, H. M. Hasanien, and S. Alghuwainem, "Identification of electrical parameters for three-diode photovoltaic model using analytical and sunflower optimization algorithm," *Appl. Energy*, vol. 250, pp. 109–117, Sep. 2019.
[6] G. Xiong, J. Zhang, X. Yuan, D. Shi, Y. He, and G. Yao, "Parameter extraction of solar photovoltaic models by means of a hybrid differential evolution with whale optimization algorithm," *Sol. Energy*, vol. 176, pp. 742–761, Dec. 2018.
[7] G. Islam, S. M. Muyeen, A. Al-Durra, and H. M. Hasanien, "RTDS implementation of an improved sliding mode based inverter controller for PV system," *ISA Trans.*, vol. 62, pp. 50–59, May 2016.
[8] K. Yu, J. J. Liang, B. Y. Qu, X. Chen, and H. Wang, "Parameters identification of photovoltaic models using an improved JAYA optimization algorithm," *Energy Convers. Manage.*, vol. 150, pp. 742–753, Oct. 2017.
[9] Y. Mahmoud and E. F. El-Saadany, "A photovoltaic model with reduced computational time," *IEEE Trans. Ind. Electron.*, vol. 62, no. 6, pp. 3534–3544, Jun. 2015.
[10] H. M. Hasanien, "Shuffled frog leaping algorithm for photovoltaic model identification," *IEEE Trans. Sustain. Energy*, vol. 6, no. 2, pp. 509–515, Apr. 2015.
[11] M. F. AlHajri, K. M. El-Naggar, M. R. AlRashidi, and A. K. Al-Othman, "Optimal extraction of solar cell parameters using pattern search," *Renew. Energy*, vol. 44, pp. 238–245, Aug. 2012.
[12] L. H. I. Lim, Z. Ye, J. Ye, D. Yang, and H. Du, "A linear identification of diode models from single *I–V* characteristics of PV panels," *IEEE Trans. Ind. Electron.*, vol. 62, no. 7, pp. 4181–4193, Jul. 2015.
[13] N. M. A. Alrahim Shannan, N. Z. Yahaya, and B. Singh, "Single-diode model and two-diode model of PV modules: A comparison," in *Proc. IEEE Int. Conf. Control Syst., Comput. Eng.*, Nov. 2013, pp. 210–214.
[14] S. Gupta, H. Tiwari, M. Fozdar, and V. Chandna, "Development of a two diode model for photovoltaic modules suitable for use in simulation studies," in *Proc. Asia–Pacific Power Energy Eng. Conf.*, Mar. 2012, pp. 1–4.
[15] A. Kassis and M. Saad, "Analysis of multi-crystalline silicon solar cells at low illumination levels using a modified two-diode model," *Sol. Energy Mater. Sol. Cells*, vol. 94, no. 12, pp. 2108–2112, Dec. 2010.
[16] V. J. Chin, Z. Salam, and K. Ishaque, "Cell modelling and model parameters estimation techniques for photovoltaic simulator application: A review," *Appl. Energy*, vol. 154, pp. 500–519, Sep. 2015.
[17] K. Nishioka, N. Sakitani, Y. Uraoka, and T. Fuyuki, "Analysis of multicrystalline silicon solar cells by modified 3-diode equivalent circuit model taking leakage current through periphery into consideration," *Sol. Energy Mater. Sol. Cells*, vol. 91, no. 13, pp. 1222–1227, Aug. 2007.
[18] O. S. Elazab, H. M. Hasanien, M. A. Elgendy, and A. M. Abdeen, "Parameters estimation of single-and multiple-diode photovoltaic model using whale optimisation algorithm," *IET Renew. Power Gener.*, vol. 12, no. 15, pp. 1755–1761, Nov. 2018.
[19] D. S. Chan and J. C. Phang, "Analytical methods for the extraction of solar-cell single and double-diode model parameters from IV characteristics," *IEEE Trans. Electron Devices*, vol. ED-34, no. 2, pp. 286–293, Feb. 1987.
[20] K. Ishaque, Z. Salam, H. Taheri, and Syafaruddin, "Modeling and simulation of photovoltaic (PV) system during partial shading based on a two-diode model," *Simul. Model. Pract. Theory*, vol. 19, no. 7, pp. 1613–1626, Aug. 2011.
[21] A. A. Elbaset, H. Ali, and M. Abd-El Sattar, "Novel seven-parameter model for photovoltaic modules," *Sol. Energy Mater. Sol. Cells*, vol. 130, pp. 442–455, Nov. 2014.
[22] K. Ishaque, Z. Salam, S. Mekhilef, and A. Shamsudin, "Parameter extraction of solar photovoltaic modules using penalty-based differential evolution," *Appl. Energy*, vol. 99, pp. 297–308, Nov. 2012.
[23] M. A. Awadallah, "Variations of the bacterial foraging algorithm for the extraction of PV module parameters from nameplate data," *Energy Convers. Manage.*, vol. 113, pp. 312–320, Apr. 2016.
[24] X. Chen, K. Yu, W. Du, W. Zhao, and G. Liu, "Parameters identification of solar cell models using generalized oppositional teaching learning based optimization," *Energy*, vol. 99, pp. 170–180, Mar. 2016.
[25] D. H. Muhsen, A. B. Ghazali, T. Khatib, and I. A. Abed, "Extraction of photovoltaic module model's parameters using an improved hybrid differential evolution/electromagnetism-like algorithm," *Sol. Energy*, vol. 119, pp. 286–297, Sep. 2015.
[26] D. H. Muhsen, A. B. Ghazali, T. Khatib, and I. A. Abed, "Parameters extraction of double diode photovoltaic module's model based on hybrid evolutionary algorithm," *Energy Convers. Manage.*, vol. 105, pp. 552–561, Nov. 2015.
[27] M. R. AlRashidi, M. F. AlHajri, K. M. El-Naggar, and A. K. Al-Othman, "A new estimation approach for determining the I–V characteristics of solar cells," *Sol. Energy*, vol. 85, no. 7, pp. 1543–1550, Jul. 2011.
[28] A. Askarzadeh and A. Rezazadeh, "Parameter identification for solar cell models using harmony search-based algorithms," *Sol. Energy*, vol. 86, no. 11, pp. 3241–3249, Nov. 2012.
[29] A. Askarzadeh and A. Rezazadeh, "Artificial bee swarm optimization algorithm for parameters identification of solar cell models," *Appl. Energy*, vol. 102, pp. 943–949, Feb. 2013.
[30] D. Oliva, E. Cuevas, and G. Pajares, "Parameter identification of solar cells using artificial bee colony optimization," *Energy*, vol. 72, pp. 93–102, Aug. 2014.
[31] X. Yuan, Y. Xiang, and Y. He, "Parameter extraction of solar cell models using mutative-scale parallel chaos optimization algorithm," *Sol. Energy*, vol. 108, pp. 238–251, Oct. 2014.
[32] T. Easwarakhanthan, J. Bottin, I. Bouhouch, and C. Boutrit, "Nonlinear minimization algorithm for determining the solar cell parameters with microcomputers," *Int. J. Sol. Energy*, vol. 4, no. 1, pp. 1–12, Jan. 1986.
[33] M. S. Ismail, M. Moghavvemi, and T. M. I. Mahlia, "Characterization of PV panel and global optimization of its model parameters using genetic algorithm," *Energy Convers. Manage.*, vol. 73, pp. 10–25, Sep. 2013.
[34] A. Askarzadeh and L. dos Santos Coelho, "Determination of photovoltaic modules parameters at different operating conditions using a novel bird mating optimizer approach," *Energy Convers. Manage.*, vol. 89, pp. 608–614, Jan. 2015.
[35] S. Talatahari and M. Azizi, "Chaos game optimization: A novel metaheuristic algorithm," *Artif. Intell. Rev.*, vol. 54, no. 2, pp. 917–1004, Feb. 2021.
[36] K.-I. Kurobe and H. Matsunami, "New two-diode model for detailed analysis of multicrystalline silicon solar cells," *Jpn. J. Appl. Phys.*, vol. 44, no. 12, pp. 8314–8321, Dec. 2005.
[37] V. Khanna, B. K. Das, D. Bisht, Vandana, and P. K. Singh, "A three diode model for industrial solar cells and estimation of solar cell parameters using PSO algorithm," *Renew. Energy*, vol. 78, pp. 105–113, Jun. 2015.
[38] C. T. Sah, R. N. Noyce, and W. Shockley, "Carrier generation and recombination in PN junctions and PN junction characteristics," *Proc. IRE* vol. 45, no. 9, pp. 1228–1243, Sep. 1957.
[39] W. De Soto, S. A. Klein, and W. A. Beckman, "Improvement and validation of a model for photovoltaic array performance," *Sol. Energy*, vol. 80, no. 1, pp. 78–88, Jan. 2006.
[40] Z. Yan, L. Chunquan, S. Zhenshou, L. Xiong, and A. C. Luo, "An improved brain storming optimization algorithm for estimating parameters of photovoltaic models," *IEEE Access*, vol. 7, pp. 77629–77641, 2019.
[41] M. H. Hassan, S. Kamel, M. A. El-Dabah, and H. Rezk, "A novel solution methodology based on a modified gradient-based optimizer for parameter estimation of photovoltaic models," *Electronics*, vol. 10, no. 4, p. 472, Feb. 2021.
[42] A. Ramadan, S. Kamel, A. Korashy, and J. Yu, "Photovoltaic cells parameter estimation using an enhanced teaching–learning-based optimization algorithm," *Iranian J. Sci. Technol., Trans. Electr. Eng.*, vol. 44, no. 2, pp. 767–779, Jun. 2020.